

Collective excitations in the normal state of Cu-O-based superconductors

P. B. Littlewood, C. M. Varma, and S. Schmitt-Rink
AT&T Bell Laboratories, Murray Hill, New Jersey 07974

E. Abrahams

Serlin Physics Laboratory, Rutgers University, Piscataway, New Jersey 08855
 (Received 27 December 1988)

Standard weak-coupling methods are used to calculate the excitation spectrum and the instabilities of the metallic phase of a three-band model for the copper-oxide superconductors with both intra- and intersite repulsion. Besides the magnetic excitations, a strong charge-transfer resonance of A_{1g} symmetry is predicted. For reasonable parameters, the metallic phase is found to be unstable to a charge-transfer instability at large deviations from half filling, and at small deviations to an antiferromagnet.

One of the questions for the understanding of the high- T_c Cu-O-based superconductors is the spectral function for effective electron-electron interactions. Towards this end, in this paper we calculate the collective excitations of a model for CuO_2 planes based on weak-coupling methods. If the metallic phase of the Cu-O materials, extrapolated to low temperatures, is a Fermi liquid,¹ standard weak-coupling methods should give a qualitatively correct description of the ground and excited states. In such a case, it is probable that low-lying electronic excitations, of charge or spin character, play an essential dynamical role in the superconductive pairing mechanism. Even if the metallic phase is not a Fermi liquid, the high-energy excitations calculated here should still be pertinent, and the calculated low-energy excitations can indicate possible instabilities of the metallic phase. Weak-coupling methods are, of course, inappropriate in the undoped material with its antiferromagnetic (AFM) ground state.² However, even in that case, these calculations do provide an indication of the instability of the Fermi-liquid phase to such a state.

Consequently, it is of interest to carry out weak-coupling calculations to obtain the excitation spectrum and phase diagram in a model of CuO_2 planes which incorporates features essential and unique to the Cu-O superconductors. In what follows, we describe the model, sketch the calculations (which are based on standard methods), and discuss the results.

We use a Hamiltonian for the CuO_2 planes in a tight-binding basis which is an extended Hubbard model defined on the $d_{x^2-y^2}$ orbital for Cu and $(\sigma)p_x$ orbital on one of the two O atoms in the unit cell and the $(\sigma)p_y$ orbital on the other³

$$\begin{aligned}
 H = & \epsilon \sum_i (c_{di}^\dagger c_{di} - c_{xi}^\dagger c_{xi} - c_{yi}^\dagger c_{yi}) \\
 & + \sum_{\langle ij \rangle} (t_{ij} c_{di}^\dagger c_{xj} + \text{H.c.} + x \rightarrow y) \\
 & + \frac{1}{2} U \sum_i \delta n_{di} \delta n_{di} + V \sum_{\langle ij \rangle} \delta n_{di} (\delta n_{xj} + \delta n_{yj}).
 \end{aligned}$$

Here $\epsilon = \frac{1}{2} (E_d - E_p)$, $t_{ij} = \pm t$, and we have included a repulsive U on Cu as well as the nearest-neighbor repul-

sive V . The notation $\langle ij \rangle$ specifies nearest-neighbor summation. The band parameters ϵ and t are defined in the Hartree-Fock approximation, and $\delta n_i = n_i - \langle n_i \rangle$. We have neglected repulsion on the O atom as well as direct O-O hopping. They introduce no new qualitative features in the present calculation (although they may be important for superconductivity), and results including their effects will be presented later. Equation (1) yields three bands, with the uppermost antibonding band half-filled for the $d^9 p^6$ configuration. Self-consistent band-structure calculations reveal that there is strong admixture of Cu and O orbitals, with $\epsilon \sim 0$,⁴ and photoemission experiments in the insulating phase show that the lowest-charge excitation has a strong O to Cu charge-transfer character.⁵ Under these circumstances, as noted elsewhere,³ the longer-range electronic interactions, which stabilize the ionic structures to begin with, and which are parametrized in the model by V , have an important *dynamical* role to play.

The model exhibits several different phases depending upon the values of ϵ , U , V (in units of t) and of the number of holes δ (measured from half-filling). As we discuss below, in addition to the expected spin-density-wave (SDW) and charge-density-wave (CDW) phases which occur for low doping, we find a new charge-transfer instability (CTI) of the metallic state. Whereas the CDW and SDW instabilities are driven by $q \sim \pi$ intraband excitations (and are suppressed by doping) the CTI is driven by $q \sim 0$ interband transitions which are dramatically softened by the excitonic effect of the intersite coupling V (and are enhanced by doping).

We first construct the Bethe-Salpeter equation for the particle-hole propagator $P_{\alpha\beta\beta'\alpha'}^\pm(k, k', q)$, including both direct and exchange scattering (see Fig. 1). Here $\alpha\beta \dots$ are the orbital indices, and the superscript \pm refers to

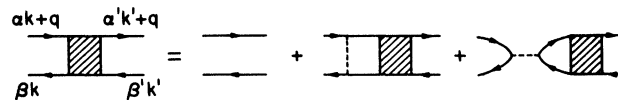


FIG. 1. Diagrammatic representation of the Bethe-Salpeter equation for the particle-hole propagator $P_{\alpha\beta\beta'\alpha'}^\pm(k, k', q)$.

charge and spin channels. The equation for P is complicated by the nonlocality of the exchange interaction, but enormous simplification results because the interactions can be written as separable functions of the form

$$V_{\alpha\beta\beta'\alpha'}^{D,X}(\mathbf{k}+\mathbf{q},\mathbf{k},\mathbf{k}',\mathbf{k}'+\mathbf{q}) = \sum_{i,j} g_{\alpha\beta}^i(\mathbf{k},\mathbf{k}+\mathbf{q}) V_{D,X}^{ij}(\mathbf{q}) g_{\alpha'\beta'}^j(\mathbf{k}',\mathbf{k}'+\mathbf{q}). \quad (2)$$

Here D, X refer to direct and exchange channels, and the functions g^i form a basis for particle-hole pair wave functions. The integral equation reduces to solving for the generalized polarizability matrix

$$P_{ij}(\mathbf{q},\omega) = \sum_{\alpha\beta\beta'\alpha'} \sum_{kk'} g_{\alpha\beta}^i(\mathbf{k}+\mathbf{q},\mathbf{k}) P_{\alpha\beta\beta'\alpha'}(k,k',q) \times g_{\alpha'\beta'}^j(\mathbf{k}'+\mathbf{q},\mathbf{k}'), \quad (3)$$

with $k=(\mathbf{k},k_0)$, $q_0=\omega$ which is of dimension (11×11) in this case. Note that by using a tight-binding basis and the separability of the resulting interactions, local-field effects for the model are exactly included in the solution; P^{ij} is a real-space representation of the dielectric matrix $\epsilon(\mathbf{q}+\mathbf{G},\mathbf{q}+\mathbf{G}',\omega)$ in reciprocal space.

P can be separated into the charge- and spin-fluctuation channels straightforwardly, leading to the matrix equations (all indices are suppressed) $P^\pm = D^\pm P_0$, where $P_0(\mathbf{q},\omega)$ is the bare "bubble," and we have introduced propagators for charge and spin fluctuations

$$[D^+]^{-1} = I + P_0(V_X - 2V_D), \quad (4a)$$

$$[D^-]^{-1} = I + P_0V_X. \quad (4b)$$

Here I is the unit matrix. The spectral representation of these operators yields the particle-hole spectrum including exchange and local-field corrections, and is a generalization of the methods used by Hanke and Sham and by Sinha *et al.* in other contexts.⁶ Were only the spin-fluctuations kept, this would be equivalent to the paramagnon theory,⁷ and some recent calculations on the single-band Hubbard model have followed this approach.⁸

Zeros of the operators D^\pm give the energy spectrum of collective modes. At $\mathbf{q}=0$ in the charge channel, we distinguish different modes by their symmetry, and in Fig. 2 we plot their energies as a function of band filling $n = \frac{1}{2}(1-\delta)$ for some representative values of parameters. Spectral weight for nonbonding (σ^0) to antibonding (σ^*) transitions begins at an energy $\lesssim 2t$ and for bonding (σ) to antibonding transitions at an energy $\lesssim 4t$ in the band structure. At an energy just below the $\sigma^0 \rightarrow \sigma^*$ onset, two excitonic states [$B_{1g}(x^2-y^2)$ and $E_u(x,y)$] are split off weakly. The state of $A_{1g}(x^2+y^2)$ symmetry garners its oscillator strength from $\sigma \rightarrow \sigma^*$ transitions at energies $\gtrsim 4t$ and is pulled far down below the band edge for moderate values of V/t . Note that the only optically-active transitions are the E_u dipole active modes (dotted line in the figure). Because we have used Hartree-Fock single-particle Green's functions in the evaluation of P_{ij} , these excitonic modes are undamped as long as they lie outside the particle-hole continuum.

It is important to remember that the single-particle spectrum is renormalized by interaction with the collective modes. In Fig. 3 we show the single-particle spectral

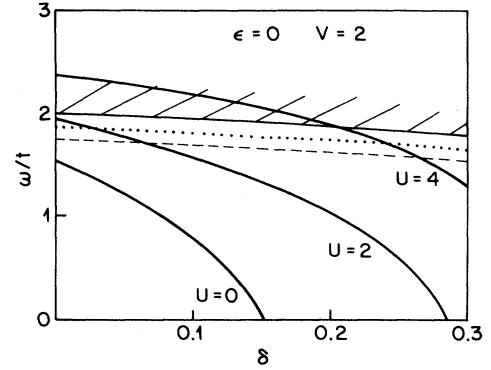


FIG. 2. Energies of charge-fluctuation collective modes at $\mathbf{q}=0$ for $\epsilon=0$, $V/t=2$, $U/t=0,2,4$. Solid lines: A_{1g} ; dashed line: B_{1g} ; dotted line: E_u . (The B_{1g} and E_u modes are insensitive to U .) The hatched regions mark the onset of interband transitions.

weight $A(\mathbf{p},\nu) = \text{Tr Im}[\nu - H_0 - \Sigma(\mathbf{p},\nu)]$ with the self-energy evaluated to second order in perturbation theory for momenta $\mathbf{k}=(\zeta,\zeta)$. The free-particle bands become damped, so that quasiparticles off the Fermi surface at $\nu=0$ acquire a finite lifetime. The bands are also narrowed, i.e., there is an effective-mass enhancement as a result of interaction with the collective modes. The "band" which has developed at energies above E_f is the "upper Hubbard (or charge transfer) band" produced by correlations on the Cu sites as well as a renormalization of the average gap for charge-transfer excitations. An effect of V in this model is to shift 0 spectral weight in the non-bonding band up toward E_f . We shall present more detailed results on the single-particle spectrum elsewhere.

As well as the $q=0$ particle-hole spectrum shown in Fig. 2, there is, of course, spectral weight at finite q . In

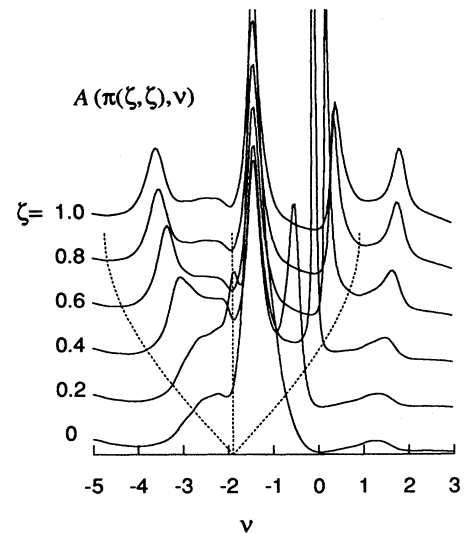


FIG. 3. Electron spectral function $A(\mathbf{p},\nu)$ for a set of momenta $\mathbf{p}=\pi(\zeta,\zeta)$, and $\epsilon=0$, $\delta=0.2$, $U/t=2$, $V/t=1$. The dashed lines mark the positions of unrenormalized bands, and energies are measured relative to E_f .

both charge and spin channels, the large q spectral weight at low frequency ($\omega \ll t$) is dominated by intraband excitations across the Fermi surface. Because the Fermi surface is well nested (close to $\delta=0$) these fluctuations are strongly enhanced; in fact, at small values of U or V these modes may become soft, leading to a SDW or CDW instability. Close enough to the instability of the metallic state, either of these processes gives rise to large renormalizations of the single-particle behavior familiar from the usual paramagnon theory.⁷

With the neglect of O-O hopping, at half-filling the metallic state is unstable to either a SDW or to a CDW for infinitesimal Coulomb repulsion. For nonzero doping δ , this instability is suppressed and the metallic state has a finite range of stability. In Fig. 4, we show the calculated phase boundaries to either SDW (for $V=0$, dashed line) or CDW (for $U=0$, dotted line). These instabilities are suppressed as soon as self-energy corrections are taken into account, and in Fig. 4 we also plot the stability region of the metallic paramagnetic state including self-energy corrections to second order in the interactions.⁹ The three surfaces in the figure mark the onset of SDW, CDW, and CTI, determined by the appearance of a zero eigenvalue of one of the operators $[D^\pm(\mathbf{q}, \omega=0)]^{-1}$. In the cases of SDW and CDW these instabilities occur at finite \mathbf{q} , whereas the CTI corresponds to the softening of the A_{1g} mode shown in Fig. 2, at $\mathbf{q}=0$. As the eigenvector for this mode corresponds to a symmetric charge oscillation be-

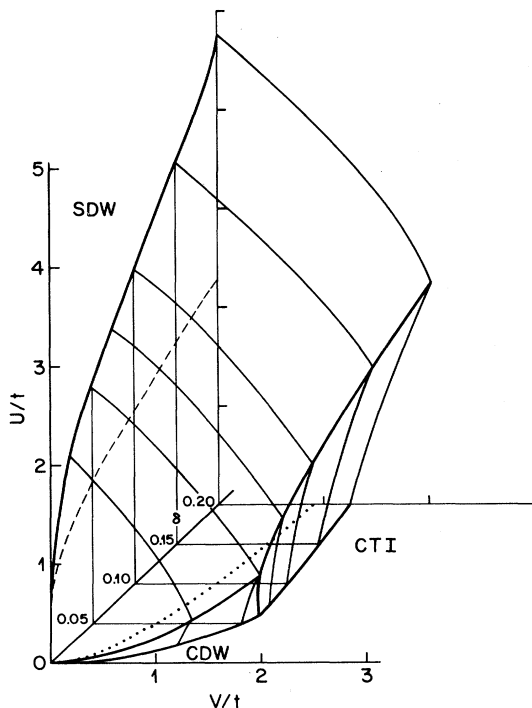


FIG. 4. Stability region of metallic paramagnetic state as a function of doping (δ), intrasite (U), and intersite (V) Coulomb interaction. The three surfaces mark the instabilities to SDW, CDW, or CTI. The dashed line ($V=0$ plane) and dotted line ($U=0$ plane) mark the calculated instabilities to SDW and CDW, respectively, when self-energy corrections are neglected.

tween Cu and O neighbors, its instability signals a valence change from the assumed value. We note that for values of $\delta \gtrsim 0.05$ the inclusion of moderate O-O hopping does not significantly affect the phase diagram of Fig. 4.

It is tempting to associate the charge-transfer instability in Fig. 4 with the observation that in all known Cu-O superconductors, doping beyond a certain deviation from half-filling is not possible,¹⁰ and that the maximum T_c 's are obtained close to this point. We speculate that the valence change at the CTI might correspond to the disintegration of the lattice structure,¹¹ and we believe that the CTI is the same instability as that identified as phase separation in calculations performed in the strong coupling limit.¹²

Figure 5 shows the calculated spectral function $\text{Im}D^+(\mathbf{q}=0, \omega)$ decomposed into different symmetries, again with second-order self-energy corrections which lead to a finite lifetime for the modes.^{9,13} Here the strongest feature is the A_{1g} mode, which for these parameters is the lowest $\mathbf{q}=0$ excitation.

Optical experiments¹⁴ on single-crystal $\text{YBa}_2\text{Cu}_3\text{O}_{7-\delta}$ have shown the presence of a strong broad feature in the mid-ir; furthermore, in the energy range $0 < \omega \lesssim 1.5$ eV, the oscillator strength is somewhat larger than can be easily accounted for on the basis of intraband transitions. If this feature is associated with the CuO_2 planes, it is possible that defects, or even metallic fluctuations, break the A_{1g} symmetry and allow the lowest CTR mode to acquire optical activity. The coupling of the A_{1g} mode to Drude transitions will also modify the form of $\sigma(\omega)$ by generating an energy-dependent lifetime and effective mass for the quasiparticles.¹⁵ Recent measurements on $\text{La}_{2-x}\text{Sr}_x\text{CuO}_4$ thin films¹⁶ have revealed a sharp absorption peak in the doped metals ($x > 0$) at energies (~ 1.5 eV) comparable to the absorption edge in the insulator ($x=0$). This might be interpreted as the E_u symmetry excitations in Fig. 5, with the sharpness of the feature indicating the strength of longer-range Coulomb interactions. Raman experiments would yield the clearest test of this model, and some recent experiments in $\text{La}_{2-x}\text{Sr}_x\text{CuO}_4$ have shown resonance enhancements of two-phonon

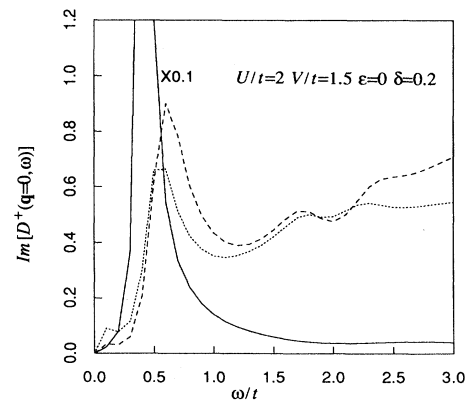


FIG. 5. Spectral representation of the charge-fluctuation propagator $\text{Im}D^+(\mathbf{q}=0, \omega)$ projected onto excitations of different symmetry (dotted line: dipole active; solid line: A_{1g} ; dashed line: B_{1g}).

lines which indicate the presence of an even symmetry mode at an energy $\sim 2-2.5$ eV.^{17,18} In both insulating and superconducting samples of $\text{Ba}_2\text{YCu}_3\text{O}_{7-\delta}$ there exists A_{1g} oscillator strength at low energies¹⁸ which is not obviously accounted for by spin fluctuations, and which also shows resonant behavior.

In conclusion, we have outlined a calculational scheme by which the effects of both spin and charge fluctuations can be treated on an equal footing in the metallic state. The values of Coulomb parameters that can be explored reliably with weak-coupling techniques are not far removed from values estimated by several authors ($U/t \sim 8$, $V/t \sim 1$).¹⁹ Moderate intersite-Coulomb interaction is found to lead to a strongly bound resonance of A_{1g} symmetry, while the optically active spectrum is shifted only weakly from the particle-hole continuum. Charge-

transfer resonances were suggested as a possible pairing mechanism;³ some recent calculations based on Eq. (1) with $V/t \sim 1$ support this point of view.^{12,20} Our calculation also generates effective interactions between quasi-particles via Eq. (4), which can be used to test models of either charge- or spin-fluctuation mediated pairing. Further work on the pairing instabilities is in progress and will be reported elsewhere.

The authors would like to thank P. A. Fleury, K. B. Lyons, and P. A. Sulewski for a number of discussions, and I. Ohana and D. Heiman for communicating results prior to publication. We also acknowledge several discussions with S. N. Coppersmith on many aspects of this work.

¹This matter is addressed by recent experiments, but has not been conclusively settled. See A. Bansil *et al.*, Phys. Rev. Lett. **61**, 2480 (1988); L. Hoffmann *et al.*, Europhys. Lett. **6**, 61 (1988).

²D. Vakinin *et al.*, Phys. Rev. Lett. **58**, 2802 (1987); G. Shirane *et al.*, *ibid.* **59**, 1613 (1987).

³C. M. Varma, S. Schmitt-Rink, and E. Abrahams, Solid State Commun. **62**, 681 (1987); and in *Novel Mechanisms of Superconductivity*, edited by V. Kresin and S. Wolf (Plenum, New York, 1987), p. 355.

⁴L. F. Mattheiss, Phys. Rev. Lett. **58**, 1028 (1987).

⁵See the section on spectroscopy in *High Temperature Superconductors*, edited by J. Müller and J. L. Olsen (North-Holland, Amsterdam, 1988).

⁶W. R. Hanke and L. J. Sham, Phys. Rev. B **12**, 4501 (1975); S. K. Sinha, R. P. Gupta, and D. L. Price, *ibid.* **9**, 2564 (1974).

⁷We note that for the pure Hubbard model ($V=0$) all matrices are replaced by scalars (only the dd channel need be kept) and the charge- and spin-fluctuation propagators are simply given by the conventional result $D^\pm = [1 \mp UP_0]^{-1}$. See, e.g., S. Doniach and S. Engelsberg, Phys. Rev. Lett. **17**, 750 (1966).

⁸N. E. Bickers *et al.*, Bull. Am. Phys. Soc. **33**, 452 (1988).

⁹We have *not* made vertex corrections to the same order as the self-energy corrections, so the approximation for $D(\mathbf{q}, \omega)$ is not conserving. However, the errors in the sum rule are $\lesssim 50\%$ over the range of U, V, δ in Fig. 4, and the qualitative appearance of the phase diagram should be unchanged. In particular, the CTI is not strongly affected by the inclusion of self-energy corrections, as its oscillator strength is derived from high-energy $\gtrsim 4t$ single-particle transitions.

¹⁰A. W. Sleight *et al.*, in *Chemistry of High Temperature Superconductors*, edited by D. L. Nelson, M. S. Whittingham,

and T. F. George (American Chemical Society, Washington, D.C., 1987); C. M. Varma, in *International Discussion Meeting on High Temperature Superconductors*, edited by H. W. Weber (Plenum, New York, 1988).

¹¹The softening of this mode would lead to anomalies in the bulk modulus; certainly any real transition would be first order and would set in before $\omega_{A_{1g}} \rightarrow 0$.

¹²J. E. Hirsch *et al.* (unpublished); S. A. Trugman (unpublished); S. N. Coppersmith (unpublished).

¹³A decay mode for the charge-transfer resonance, not considered by us, is the decay into two particle-hole intraband excitations which arises from the neglected vertex corrections and will lead to further broadening of the resonance.

¹⁴D. A. Bonn *et al.*, Phys. Rev. B **37**, 1574 (1988); G. A. Thomas *et al.*, Phys. Rev. Lett. **61**, 1313 (1988).

¹⁵We note, however, that calculations using a second-order Holstein process were not able to reproduce both the frequency and temperature dependence observed; see Thomas *et al.* (Ref. 14).

¹⁶M. Suzuki (unpublished).

¹⁷W. H. Weber *et al.*, Phys. Rev. B **38**, 917 (1988); S. Sugai, S. Shamoto, and M. Sato, *ibid.* **38**, 6436 (1988); I. Ohana and D. Heiman (unpublished).

¹⁸K. B. Lyons, P. Sulewski, and P. A. Fleury (unpublished).

¹⁹E. B. Stechel and D. R. Jennison, Phys. Rev. B **38**, 4632 (1988); A. K. McMahan, R. M. Martin, and S. Satpathy, *ibid.* **38**, 6650 (1988); M. S. Hybertsen, M. Schlüter, and N. E. Christiansen (unpublished).

²⁰J. E. Hirsch *et al.*, Phys. Rev. Lett. **60**, 1668 (1988); C. A. Balseiro *et al.* (unpublished); M. D. Nunez Regueiro and A. A. Aligia, Phys. Rev. Lett. **61**, 1889 (1988); W. H. Stephen *et al.* (unpublished).